A POLARIMETRIC MODEL OF TOPOGRAPHIC EFFECTS ON P-BAND FOREST BACKSCATTER

Erik Blomberg, Maciej J. Soja, and Lars M. H. Ulander

Chalmers University of Technology, 412 96 Gothenburg, Sweden

ABSTRACT

P-band backscatter from boreal forest is simulated using a fully polarimetric Cylinder-Over-Ground model. Trees are represented by tapered stacks of cylinders placed over lossy dielectric planar ground that is individually fitted to the topography. The results show a strong topographic dependence and also demonstrate the limitations of the odd-, even, and volume-scattering interpretation of the Pauli decomposition. BioSAR 3 SAR images, *in-situ* data and LiDAR-derived DCM and DTM enable a comparison with real forest backscatter through simulation of complete plots. While many features are reproduced the need for an expansion of the model to include ground and branch scattering is identified. If sufficient agreement is achieved the model will be used to further improve topographic corrections for the retrieval of above ground forest biomass from P-band SAR images.

Key words: forest backscatter, topography, modelling, P-band, synthetic aperture radar (SAR).

1. INTRODUCTION

BIOMASS, recently selected for ESAs seventh Earth Explorer mission, will for the first time provide space based P-band SAR imagery and thereby enable global mapping of forest parameters such as biomass and tree height. Several data collection campaigns were conducted to support the proposal, such as BioSAR, concentrating on boreal forest at two test sites in Sweden, and TropiSAR, focusing on tropical forest in French Guiana. These have provided forest and airborne P-band SAR data which have been used to demonstrate how this novel resource can be used to estimate relevant forest parameters [1, 2, 3, 4].

It has been observed in P-Band polarimetric SAR images that the backscatter is significantly affected by the local topography, likely due to the strong stem ground double bounce contribution. This can interfere with the retrieval of biomass from P-band SAR - for example, good accuracy biomass estimation has been achieved using a polarimetric regression model which requires information about the ground slope angle [1, 3].

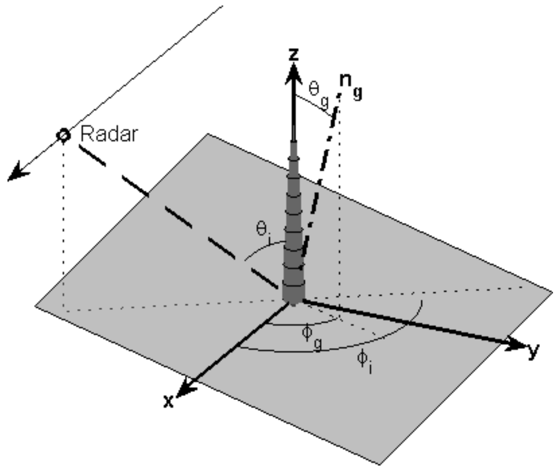

Figure 1: A tapered stack of 10 cylinders representing a single stem on sloping ground.

It is therefore desirable to further examine the impact of topography on the forest backscatter, especially for the different polarization components. Previous work using polarimetric electromagnetic modelling has produced significant variations in P-band backscatter from boreal forest if a local topography is included. A physical-optics based model incorporating a detailed undulating ground showed that these effects are important down to sub-plot dimensions [5]. This level of modelling is computationally unpractical, however preliminary results from the less demanding Cylinder-Over-Ground model presented in [6] confirm these findings.

This paper presents results from the ongoing work of improving and evaluating this model, including an update of simulations using BioSAR 3 data as input.

2. CYLINDER-OVER-GROUND MODEL

The model, described in detail in [6], is based on a modelling effort relating to the CARABAS airborne SAR system [7]. This was adapted to P-band (from low VHF-band) and simulates cylinders over a lossy dielectric infinite ground using the truncated infinite cylinder approximation. The polarimetric components of the di-

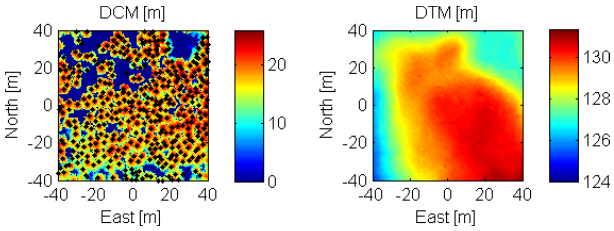

(a) Plot 1010.

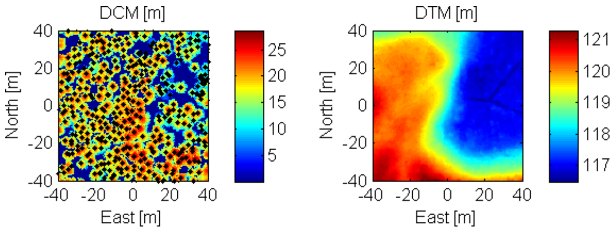

(b) Plot 1017.

Figure 2: DCM with individual tree positions and DTM for the two 80 m by 80 m plots.

rect, double bounce and triple bounce contributions to the backscatter are calculated for each cylinder and coherently added, with higher order interactions (such as shadowing) being omitted for simplicity. All cylinders are independently sized, positioned and oriented with respect to an corresponding ground plane. This allows for tree stems to be modeled as tapering stacks of cylinders with varying topography for each tree, see Figure 1 on the preceding page.

3. BIOSAR 3 DATA

BioSAR 3 was the third in a series of ESA funded campaigns focused on evaluating P-band SAR acquisitions from hemi-boreal forest in support of the upcoming BIOMASS mission. The campaign took place in the Remnngstorp test site in the south of Sweden (58 30 N, 13 40E) in 2010 as a follow up and expansion of BioSAR 1 in 2007. It involved the collection of P- and L-band SAR images as well as extensive *In-situ* measurements and LiDAR acquisitions covering most of the site [8].

3.1. LiDAR and *In-situ* data

Available LiDAR-derived data consist of a site-wide digital topography model (DTM) and digital canopy model(DCM) in a 0.5 m by 0.5 m raster. These were acquired using the TopEye MkIII helicopter-borne system and are in this work used to provide topography (DTM) and tree height (DCM).

In-situ data were collected from several different plots, some of which were combined with the LiDAR data to provide biomass maps of the site. The data used in this

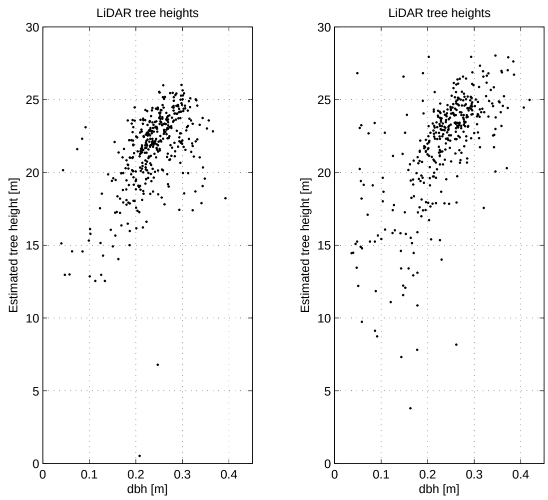

(a) Plot 1010. (b) Plot 1017.

Figure 3: DCM derived tree height as a function of dbh.

paper is from two 80 m by 80 m plots (1010 and 1017) for which the position and diameter at breast height (dbh) of every tree (with a dbh greater than 5 cm) are available.

Figure 2 shows these data for the two plots. Ground slopes used in the simulations were calculated from the DTM. The plots were selected due to their marked topographic features in combination with having a similar range of incidence angles for the different radar acquisitions.

Tree heights were obtained by querying the DCM at the tree positions, resulting in estimates seen in Figure 3. There are some outliers, mostly involving exaggerated heights for smaller dbh values - as expected from small trees being overshadowed by larger neighbours. A weighting could be performed to approach the distribution expected from allometric relationships, but the errors present were not considered significant for low level simulations.

3.2. SAR images

SAR images were obtained in September in a left looking geometry at both P- and L-band for different headings as well as tomographic baselines. The radar system used was the ONERA SETHI airborne SAR with a bandwidth, in P-band, of 277-443 MHz [8]. Three images corresponding to headings 178° (looking east) through 199° to 270° (looking south) were chosen for comparison with simulation results.

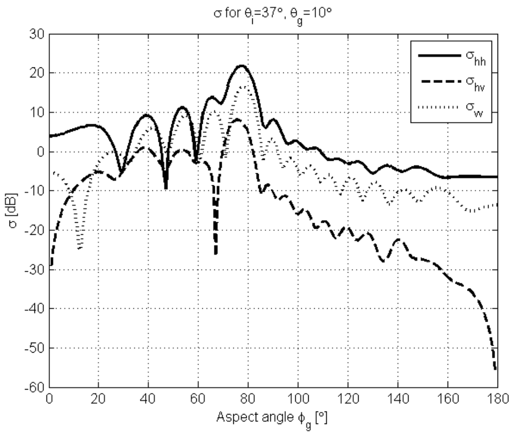

(a) Backscatter HH, HV and VV components.

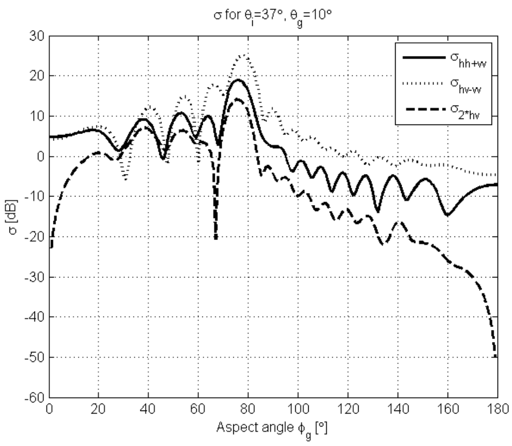

(b) Backscatter Pauli components.

Figure 4: Backscatter from from a single stem as a function of slope direction. 40 cylinders, 360 MHz, height 30 m, DBH 35 cm, $\epsilon_{r,tree} = 12.4 - 2.1i$ and $\epsilon_{r,ground} = 11.0 - 0.3i$

4. RESULTS AND DISCUSSION

All simulations used $\epsilon_{r,tree} = 12.4 - 2.1i$ and $\epsilon_{r,ground}$ and a center frequency of 360 MHz in order to be comparable to the BioSAR 3 data. Figure 4a and Figure 4b show the backscatter from a single tree on a slope of 10° for an incidence angle of 37° and different aspect angles Φ_g. This configuration is identical to the one displayed by Figure 1 on page 1 but with 40 cylinders instead of 10 to fully represent the stem profile at this wavelength (83 cm). In this case Φ_g defines the slope direction according to Figure 1 on page 1 with a mid-track incidence aspect angle $\Phi_i = 180°$, i.e. 0° being a slope towards and 180° being away from the radar track. Notable in Figure 4a is that the strongest signal for all polarisations is at an aspect angle of 70°-80° due to the slope and that the cross-polarization, while mostly lower than HH or VV, still represent a sizeable contribution for many geometries.

Figure 4b shows the in polarimetry commonly used Pauli decomposition. These components are often interpreted as representing the contributions from single, double bounce and volume scattering mechanisms. In our case almost all of the signal is due to the double bounce which is poorly reflected in the graph where the HH-VV component is only slightly stronger.

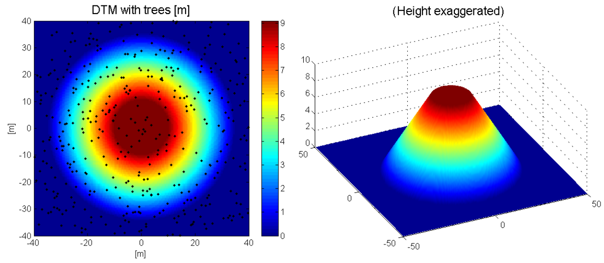

Figure 5: A hill covered with trees as represented by a truncated cone with a height of 9 m, radius of 35 m and 20° slope.

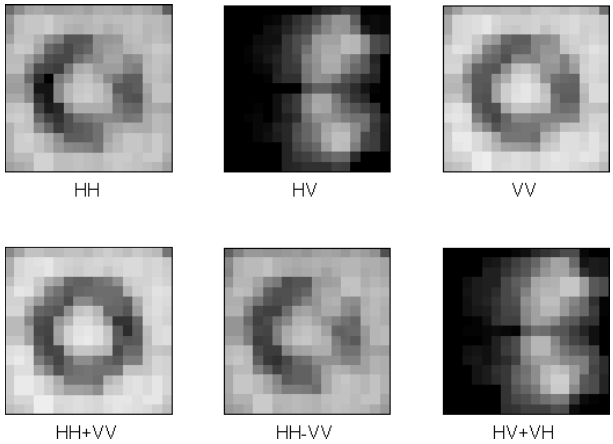

Figure 6: Simulated SAR image of the scene in Figure 5 showing HH, HV, VV and Pauli components.

These effects are demonstrated by simulating SAR returns from a forest with many stems. The example used is shown in Figure 6. 400 trees, all identical to the single stem used previously, are randomly placed on a square plot with a "hill", a 9 m high truncated cone with sides sloping a constant 20°.

The resulting SAR image is displayed in Figure 5. There is a strong return in both HH+VV and HH-VV from the flat portions due to the perfect 90° double bounce, which is greatly reduced for the slopes. The slopes facing the radar track diagonally exhibit geometries approaching a double bounce and are clearly visible, especially in HH-VV, but with a strong cross-polarization as seen in the HV images.

Having the individual tree data for plot 1010 and 1017 makes it straight forward to simulate SAR images for comparison with real radar data, as seen in Figure 7 on the next page. All images are averaged to 49 looks from the geocoded 1 m by 1 m grid and then subsampled to a 5 m by 5 grid.

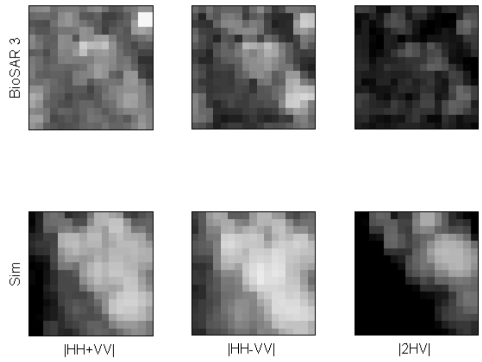

(a) Plot 1010, heading 178°.

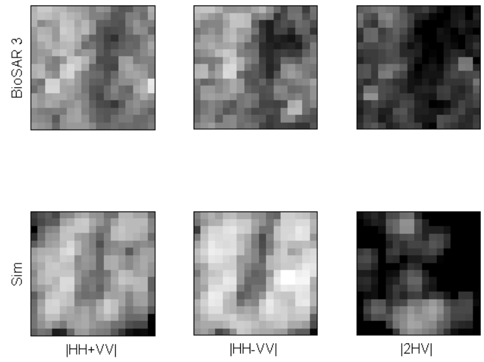

(b) Plot 1017, heading 178°.

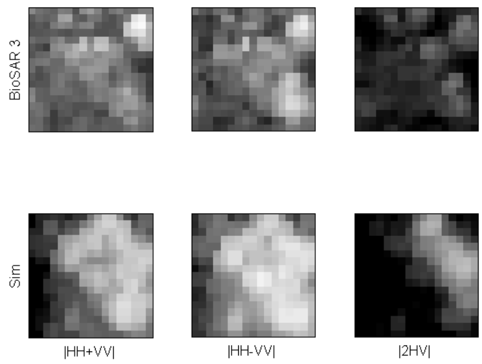

(c) Plot 1010, heading 199°.

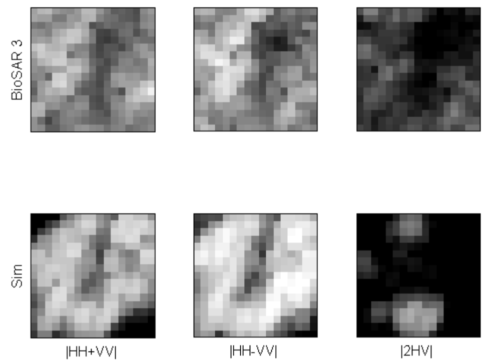

(d) Plot 1017, heading 199°.

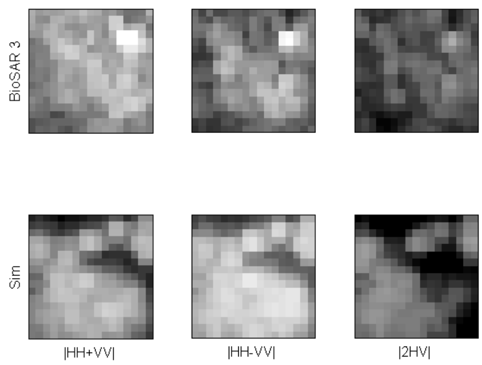

(e) Plot 1010, Heading 270°.

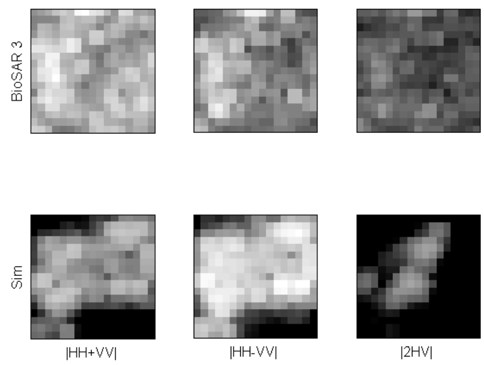

(f) Plot 1017, Heading 270°.

Figure 7: SAR data acquired during BioSAR 3 and the corresponding simulation results for plots 1010 (left) and 1017 (right) and three different flight headings (top to bottom).

Some features of the SAR data are clearly reproduced in the simulations, especially the drop in backscatter for slopes such as to the sides of plot 1010 and in the center of plot 1017. Both data and simulations show clear topographic dependence as the same scene is viewed from different directions, which is the main feature the model is meant to include.

The simulations have exaggerated contrast, which is not surprising since there is no added noise and backscatter from ground or crown volume are not included. These later omissions might also explain the much greater correlation between HV and the other channels seen in the real data as compared to the simulated results. The model will tend to maximize the difference between HV and the other components since the mechanisms giving rise to cross-polarization is different and to some extent mutually inhibiting.

5. CONCLUSIONS

Results obtained using the Cylinder-Over-Ground model are predictable and fairly easy to interpret, but the strong topographic dependence leads to excessive variations in backscatter. Future improvements will try to include direct ground returns as well as contributions from branches without to much computational burden. The expectation is that these added mechanisms will enable a close match to actual SAR images of boreal forests.

ACKNOWLEDGMENTS

The authors would like to thank ESA and all contributors for the BioSAR data and the Swedish University of Agricultural Sciences.

REFERENCES

[1] D. H. T. Minh, T. L. Toan, F. Rocca, S. Tebaldini, M. M. d'Alessandro, and L. Villard. (2014). Relating P-Band Synthetic Aperture Radar Tomography to Tropical Forest Biomass. *IEEE Transactions on Geoscience and Remote Sensing*, 52(2):967-979.

[2] G. Sandberg, L. M. H. Ulander, J. Wallerman, and J. E. S. Fransson. Measurements of forest biomass change using P-band synthetic aperture radar backscatter. (2014). *IEEE Transactions on Geoscience and Remote Sensing*, 52(10):6047-6061.

[3] M. J. Soja, G. Sandberg, and L. M. H. Ulander. (2013). Regression-based retrieval of boreal forest biomass in sloping terrain using P-band SAR backscatter intensity data. *IEEE Transactions on Geoscience and Remote Sensing*, 51(5):2646-2665.

[4] I. Hajnsek, R. Scheiber, L. M. H. Ulander, A. Gustavsson, G. Sandberg, S. Tebaldini, A. M. Guarnieri, F. Rocca, F. Bombardini, and M. Pardini. (2008). BioSAR 2007 technical assistance for the development of airborne SAR and geophysical measurements during the BioSAR 2007 experiment: Final report without synthesis. Technical report, ESA contract no. 20755/07/NL/CB.

[5] B. Hallberg, G. Smith-Jonforsen, L.M.H. Ulander, and G. Sandberg. (2008). A physical-optics model for double-bounce scattering from tree stems standing on an undulating ground surface. *IEEE Transactions on Geoscience and Remote Sensing*, 46(9):2607-2621.

[6] E. Blomberg, M. J. Soja and L. M. H. Ulander, P-bans Polarimetric Model of Vertical Tree Stems on Sloping Ground, In *IEEE International Geoscience and Remote Sensing Symposium (IGARSS)*, pages 80-83, Quebec City, QC, Canada, July 13-18 2014.

[7] G. Smith-Jonforsen, L. M H. Ulander, Xianyun Luo. (2005). Low VHF-band backscatter from coniferous forests on sloping terrain. *IEEE Transactions on Geoscience and Remote Sensing*, 43(10):2246-2260.

[8] M. H. Ulander, A. Gustavsson, B. Flood, D. Murdin, P. Dubois-Fernandez, X. Dupuis, G. Sandberg, M. J. Soja, L. E. B. Eriksson, J. E. S. Fransson, J. Holmgren and J. Wallerman. (2011). BIOSAR 2010 Technical Assistance for the Development of Airborne SAR and Geophysical Measurements during the BioSAR 2010 Experiment: Final Report, ESA contract no. 4000102285/10/NL/JA/ef.